

D-A088 152

NAVAL SURFACE WEAPONS CENTER DAHLGREN VA

F/G 11/6

SHOCK COMPRESSION OF TANTALUM.(U)

JUN 80 W MOCK, W H HOLT

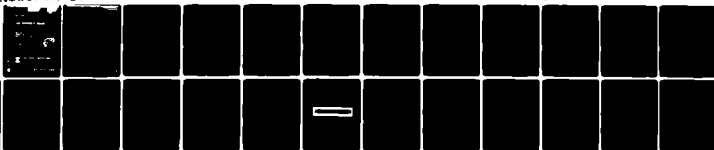
MIPR-A35200-9-0004

NCLASSIFIED

NSWC/TR-80-92

NL

20



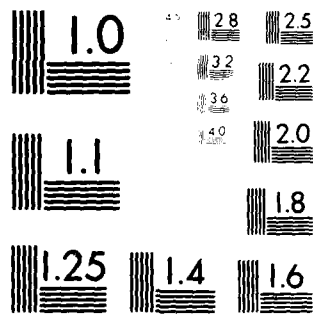
END

DATE

FILED

8-80

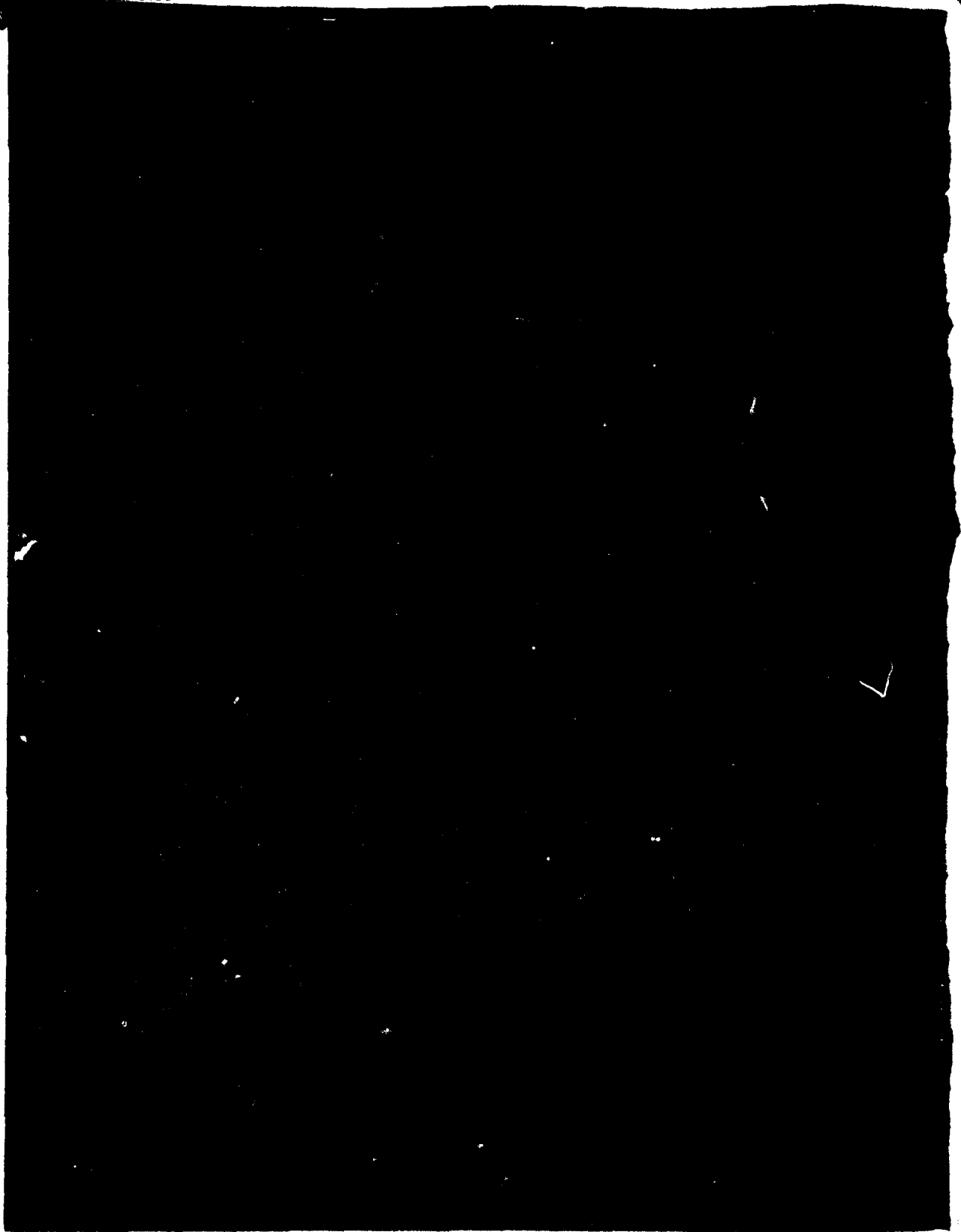
DTIC



MICROCOPY RESOLUTION TEST CHART  
 NATIONAL BUREAU OF STANDARDS-1963-A

AD A088152

00-92



UNCLASSIFIED

SECURITY CLASSIFICATION OF THIS PAGE (When Data Entered)

REPORT DOCUMENTATION PAGE		READ INSTRUCTIONS BEFORE COMPLETING FORM
1. REPORT NUMBER (17) NSWC/TR-80-92	2. GOVT ACCESSION NO. AD-A088	3. RECIPIENT'S CATALOG NUMBER 252
4. TITLE (and Subtitle) (6) Shock Compression of Tantalum	5. TYPE OF REPORT & PERIOD COVERED (9) Final Repts.	
7. AUTHOR(s) (10) Willis Mock, Jr. William H. Holt	6. PERFORMING ORG. REPORT NUMBER	
9. PERFORMING ORGANIZATION NAME AND ADDRESS Naval Surface Weapons Center Dahlgren, VA 22448	8. CONTRACT OR GRANT NUMBER(s) (15) MIPR A35200-9-0004	
11. CONTROLLING OFFICE NAME AND ADDRESS Army Engineer Waterways Experiment Station Corps of Engineers, P. O. Box 631 Vicksburg, MS 39180	10. PROGRAM ELEMENT, PROJECT, TASK AREA & WORK UNIT NUMBERS 62719A:9G95VH01	
14. MONITORING AGENCY NAME & ADDRESS (if different from Controlling Office)	12. REPORT DATE (11) June 1980	
	13. NUMBER OF PAGES 27	
	15. SECURITY CLASS. (of this report) UNCLASSIFIED	
16. DISTRIBUTION STATEMENT (of this Report)  Approved for public release; distribution unlimited.		
17. DISTRIBUTION STATEMENT (of the abstract entered in Block 20, if different from Report)		
18. SUPPLEMENTARY NOTES		
19. KEY WORDS (Continue on reverse side if necessary and identify by block number) Shock waves                      Tantalum Capacitor gauge                  Gas gun Impact                              Free-surface velocity Spall fracture		
20. ABSTRACT (Continue on reverse side if necessary and identify by block number) ➤ The free-surface velocity of a shock-loaded 3.73-mm-thick tantalum disk has been measured with a capacitor gauge. Stress reverberations were produced in the tantalum disk by impacting it with a 2.65-mm-thick alpha titanium disk at a velocity of 0.111 km/s in a gas gun. An initial shock compressive stress slightly larger than the measured 2.1-GPa Hugoniot elastic limit was produced in the tantalum. The shape of the free-surface-velocity profile suggested that spall fracture did not occur in the specimen disk at this stress level. This result was verified by examining the recovered and sectioned disk.		

DD FORM  
1 JAN 73

1473

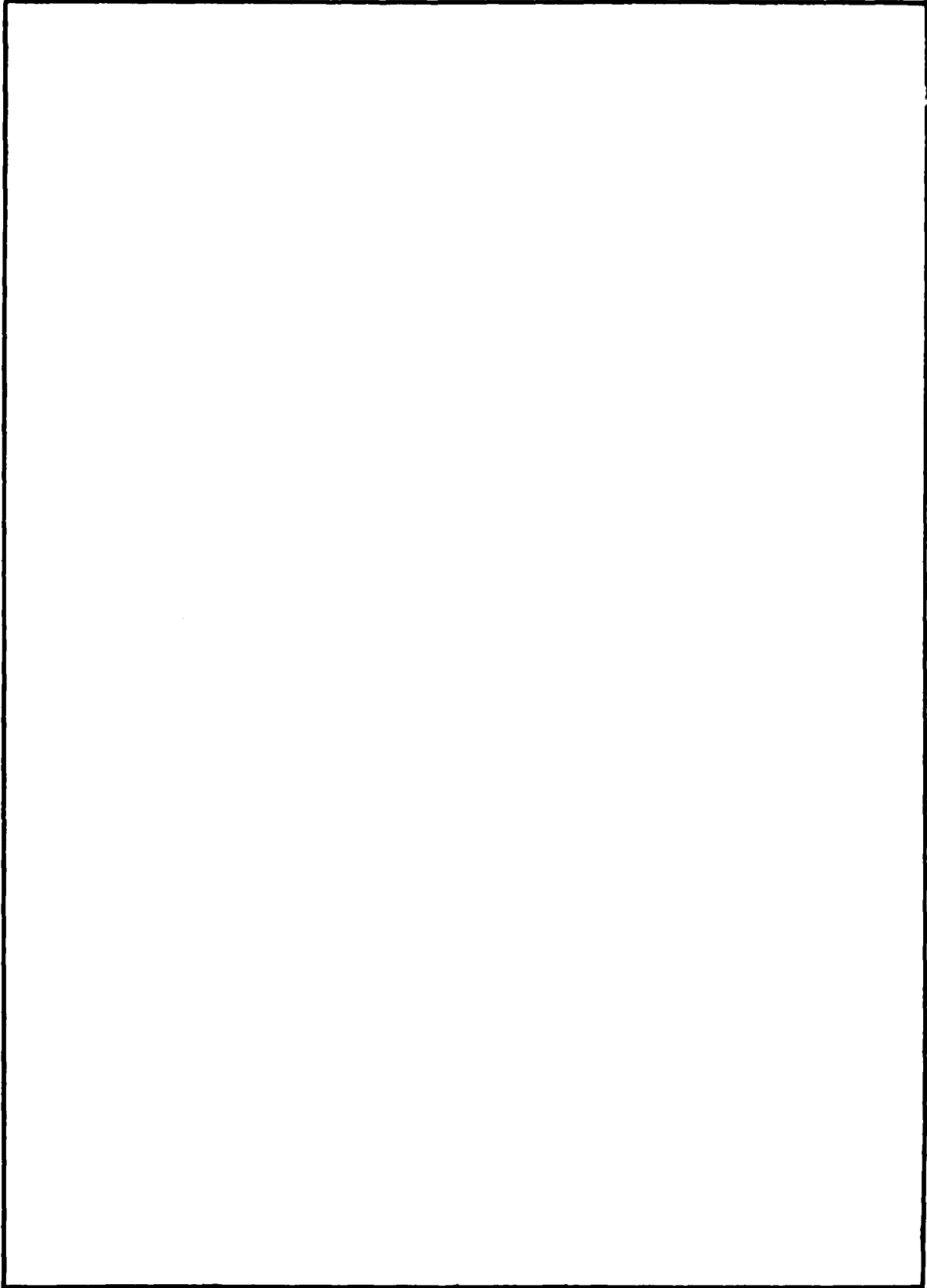
EDITION OF 1 NOV 65 IS OBSOLETE  
S/N 0102-LF-014-6601

UNCLASSIFIED

411567  
SECURITY CLASSIFICATION OF THIS PAGE (When Data Entered)

UNCLASSIFIED

SECURITY CLASSIFICATION OF THIS PAGE (When Data Entered)



UNCLASSIFIED

SECURITY CLASSIFICATION OF THIS PAGE (When Data Entered)

## FOREWORD

The capacitor gauge technique has been used to measure the shock wave compression of tantalum. This work was supported by the Army Engineer Waterways Experiment Station under MIPR No. A35200-9-0004.

This report has been reviewed and approved by C. A. Cooper, Head, Gun Systems and Munitions Division.

Released by:



CDR R. P. FUSCALDO  
Assistant for Weapons Systems  
Weapons Systems Department

Accession For	
NTIS GRA&I	<input checked="checked" type="checkbox"/>
DDC TAB	<input type="checkbox"/>
Unannounced	
Justification	
By _____	
Distribution/	
Availability Codes	
Dist	Avail and/or special
A	

## CONTENTS

	Page
I. INTRODUCTION .....	1
II. EXPERIMENTAL TECHNIQUES .....	2
III. RESULTS AND DISCUSSION .....	5
IV. SUMMARY .....	13
REFERENCES .....	14
DISTRIBUTION	



## LIST OF ILLUSTRATIONS

Figure		Page
1.	Schematic of muzzle region of gas gun showing a target assembly with a capacitor gauge. ....	2
2	Capacitor gauge calibration curve.....	4
3	Schematic of capacitor gauge and voltage limiter circuits.....	5
4	Projectile and target assembly with capacitor gauge (a) before impact and (b) after impact. ....	6
5	Oscilloscope data from target assembly with a capacitor gauge. ....	7
6	Free-surface velocity profile for the 3.73-mm-thick tantalum specimen impacted at 0.111 km/s with a 2.65-mm-thick alpha titanium impactor. ....	11
7	Photograph of the recovered, sectioned, and polished shock-loaded tantalum specimen.....	13

## LIST OF TABLES

Tables		Page
1.	Measurement of gauge capacitance versus specimen spacing.....	3
2	Digitized capacitor gauge voltage data and the corresponding free-surface-position and free-surface-velocity results for tantalum.....	10
3	Summary of shock-wave results for tantalum.....	12

## I. INTRODUCTION

The capacitor gauge technique<sup>1</sup> has been used to measure the free-surface velocity of a shock-loaded tantalum disk. Stress reverberations were produced in the specimen disk by impacting it with an alpha titanium disk of similar thickness. The first few stress reverberations in the tantalum specimen were monitored with the free-surface-velocity measurement. This type of measurement is useful for observing the effects of spall fracture in a shock-loaded disk.<sup>2</sup> Spall fracture can occur in a material if the tensile pulse produced from the interaction of rarefaction waves exceeds a threshold stress value. If the specimen fractures, the resulting spall signal influences the free-surface velocity.

A 40-mm-bore gas gun was used for shock-loading the tantalum disk.<sup>3</sup> Figure 1 is a schematic of the muzzle region of the gas gun showing a target assembly with a capacitor gauge. The time of impact is measured with four charged tilt pins which are placed around the specimen. The average projectile velocity at impact is measured with the three charged pins in the side of the barrel and the tilt pins. The free surface of the specimen forms one plate of a parallel plate capacitor. The capacitor gauge is spaced a preselected distance behind the specimen and measures the shock-induced motion of the free surface of the specimen. The shock transit time is determined by measuring the time difference between the tilt output signal and the capacitor gauge signal.

The tantalum (commercially pure grade, 99 + % purity) and alpha titanium (commercially pure grade 55, 99 + % purity) materials were purchased from Astro Metallurgical Corporation, Houston, Texas. The tantalum material was obtained in the form of 3.18- and 4.57-mm-thick plates. The alpha titanium material was obtained in the form of a 4.76-mm-thick plate. Average hardness values for machined and lapped tantalum and titanium disks are  $R_K$  52 and  $R_A$  57, respectively.<sup>4</sup>

The experimental techniques are presented in Section II. Section III contains the results and discussion. Section IV contains the summary.

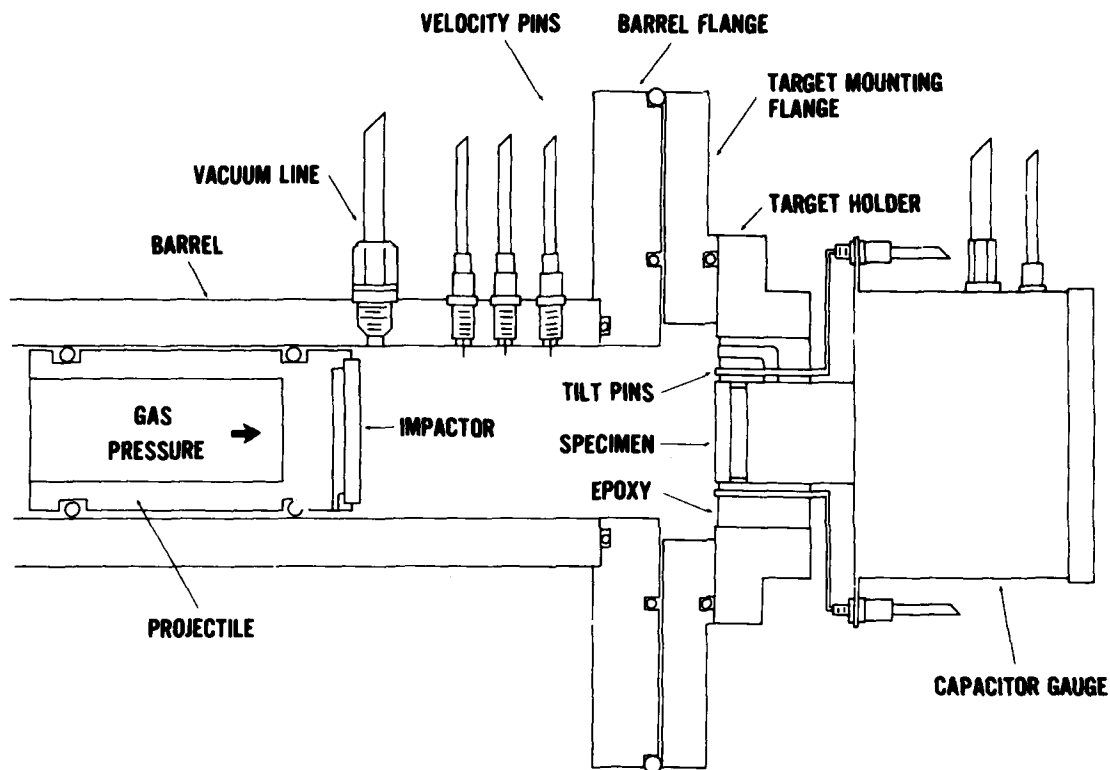


Figure 1. Schematic of muzzle region of gas gun showing a target assembly with a capacitor gauge.

## II. EXPERIMENTAL TECHNIQUES

The procedure that was used to fabricate the capacitor gauge for this experiment has been previously documented<sup>1</sup> and will not be presented here. The center conductor (Figure A-7, Reference 1) for this gauge had a diameter of 6.35 mm. The gauge was calibrated after it was assembled but prior to inserting the electrical components. The purpose of the calibration is to measure the capacitance between the center conductor and a simulated specimen face as the spacing between the specimen and center conductor is varied. A capacitance bridge system was used for the measurements (Figure 3, Reference 1). A 0.259-mm-thick spacer was used with the gauge. (This is the distance that the capacitor gauge center conductor is spaced behind the speci-

men free surface.) Beginning with the specimen spacing slightly larger than the spacer thickness, the gauge capacitance was measured as the spacing was decreased. Table 1 gives the results of the measurements. The measurements were made at a frequency of 1 kHz and had a resolution of 0.001 pF. The calibration device micrometer had a resolution of 0.002 mm.

Figure 2 is a plot of the measured gauge capacitance values versus inverse specimen spacing. The curve shown is a third-order fit to the data points using the method of least squares. The data points were also fitted with fourth-order and fifth-order curves using the method of least squares. These curves could not be distinguished from the curve in Figure 2. A second-order curve was also fitted to the data points. This curve did not fit the data points as well as the higher-order curve fits.

**Table 1. Measurement of gauge capacitance versus specimen spacing.**

Gauge Capacitance (pF)	Specimen Spacing (mm)	Gauge Capacitance (pF)	Specimen Spacing (mm)
6.163	0.269	8.371	0.114
6.212	0.259	8.534	0.109
6.274	0.249	8.810	0.104
6.336	0.239	9.035	0.099
6.405	0.229	9.387	0.094
6.482	0.219	9.711	0.089
6.565	0.209	10.211	0.084
6.672	0.199	10.553	0.079
6.761	0.189	11.287	0.074
6.883	0.179	11.951	0.069
7.018	0.169	13.044	0.064
7.178	0.159	14.128	0.059
7.362	0.149	15.936	0.054
7.579	0.139	16.805	0.052
7.827	0.129	17.203	0.051
8.145	0.119		

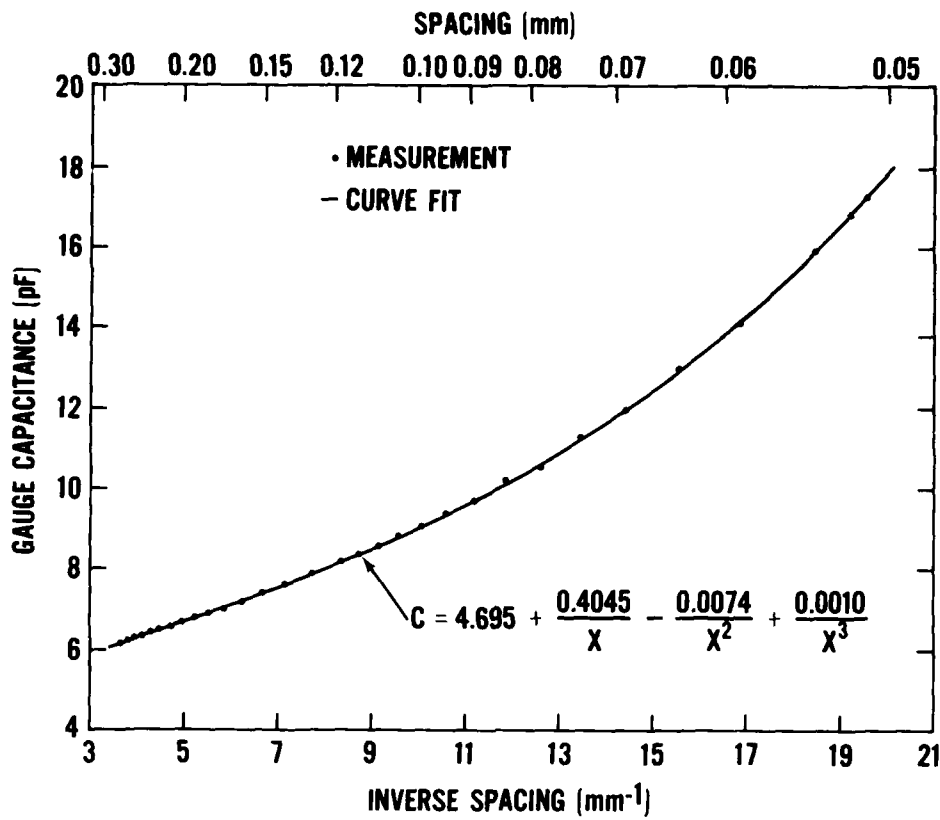


Figure 2. Capacitor gauge calibration curve. The points represent the measurements from Table 1. The calibration curve is a third-order best-fit curve; C is the gauge capacitance and x is the spacing.

After the capacitance calibration measurements were obtained, the gauge was completed by adding a 0.01- $\mu$ F coupling capacitor and a 1.5-M $\Omega$  isolation resistor to the circuit. Figure 3 shows the electrical schematic of the capacitor gauge and the voltage-limiter circuits. For this experiment the power supply voltage was set to +500 V. At projectile impact, movement of the specimen disk toward the right increases the gauge capacitance. Charge flows onto the gauge to maintain the initial voltage. The flowing charge produces a negative voltage across the 50- $\Omega$  termination resistance which is recorded on the oscilloscope. The voltage-limiter circuit protects the oscilloscope from voltage overload as the measured voltage increases.

A target assembly containing the capacitor gauge, tantalum specimen, and tilt pins was prepared using standard target preparation techniques.<sup>1,3</sup> Figure 4(a) shows the completed projectile and target assembly. The planarity of the specimen impact face was 0.3 mrad with respect to the face of the stainless steel target cup. The tilt pin ends were positioned  $4\text{ }\mu\text{m}$  above the specimen impact face. The perpendicularity of the alpha titanium impactor face to the cylindrical surface of the completed projectile was  $3\text{ }\mu\text{m}$ . Figure 4(b) shows the recovered projectile and target assembly pieces after impact.

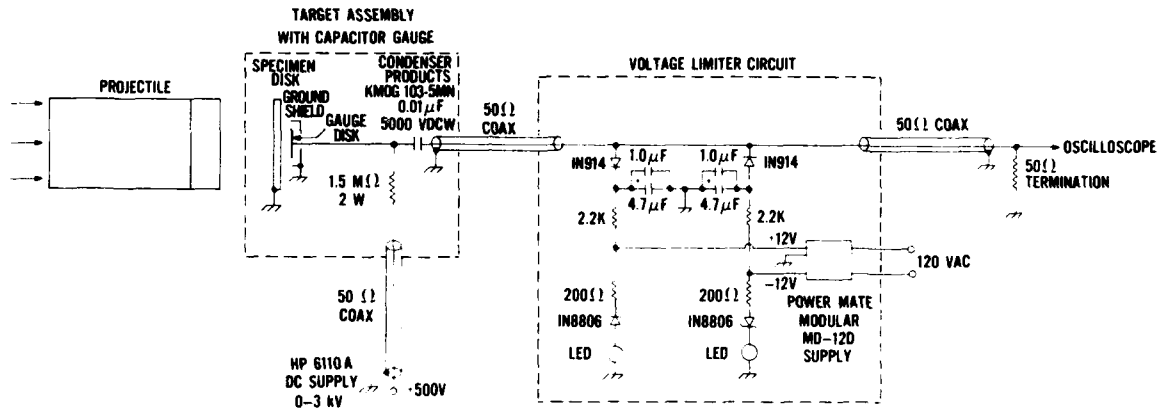


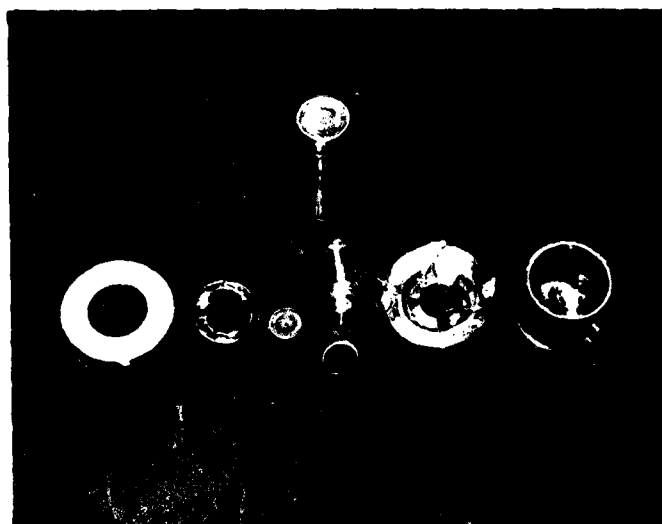
Figure 3. Schematic of capacitor gauge and voltage limiter circuits. For clarity of presentation, the tilt pins are not shown in the target assembly.

### III. RESULTS AND DISCUSSION

Figure 5 shows the tilt output and capacitor gauge oscilloscope records resulting from impacting the alpha titanium disk onto the tantalum specimen at 0.111 km/s. The impactor tilt for this shot was 0.35 mrad. The voltage-time pulse in Figure 5(b) was converted to a free-surface velocity versus time profile using the equation that describes the circuit in Figure 3 and the capacitor gauge calibration curve.

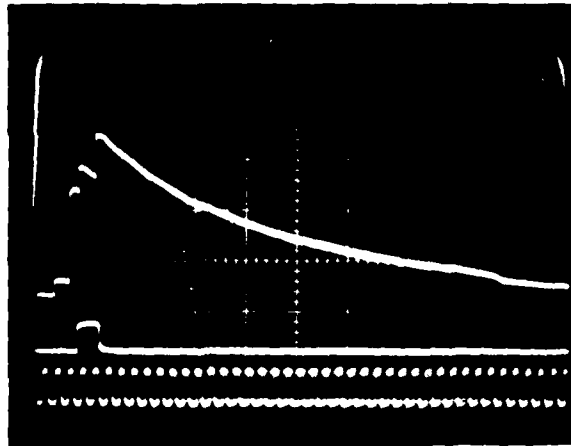


(a)

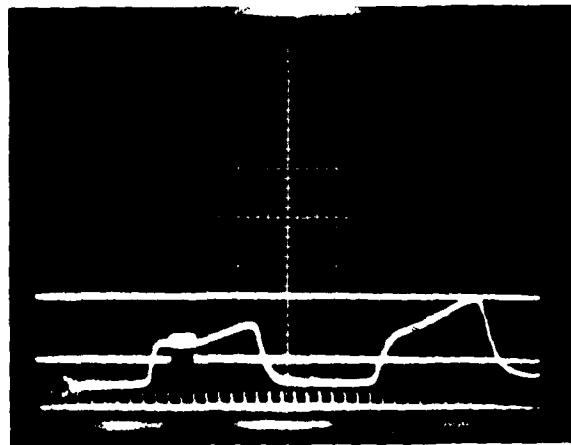


(b)

**Figure 4. Projectile and target assembly with capacitor gauge (a) before impact and (b) after impact.**



(a)



(b)

Figure 5. Oscilloscope data from target assembly with a capacitor gauge. Time increases from left to right. (a) Tilt pin data record. The vertical scale is 4 V/div. The middle trace is an initial time reference square pulse for wave velocity measurements. A 0.05- $\mu$ s-period time calibration wave is shown at the bottom. (b) Capacitor gauge data record. The vertical scale is 5 mV/div. The capacitor gauge baseline signal is shown at the top. The capacitor gauge signal (recorded in the oscilloscope reverse polarity mode) is displaced below the baseline due to a leakage current in the 0.01- $\mu$ F coupling capacitor. A 1.07- $\mu$ s delayed time reference square pulse used for the wave velocity measurements passes through the capacitor gauge signal. A 0.10- $\mu$ s-period time calibration wave is shown at the bottom.



Following Rice,<sup>5</sup> the equation describing the circuit can be approximated with

$$V(t) = -RE_0 \frac{dC}{dt} \quad (1)$$

where  $R$  is the  $50\text{-}\Omega$  termination resistance,  $V(t)$  is the measured voltage across  $R$ ,  $E_0$  is the dc capacitor gauge voltage, and  $C$  is the measured gauge capacitance. For this experiment, because of a leakage current in the  $0.01\text{-}\mu\text{F}$  coupling capacitor, a voltage less than the  $+500\text{ V}$  dc supply voltage was applied to the capacitor gauge. A leakage current value of  $183\text{ }\mu\text{A}$  was obtained using the measured  $+9.2\text{ mV}$  offset voltage in Figure 5(b). (The capacitor gauge signal was recorded in the oscilloscope reverse polarity mode.) The capacitor gauge voltage is given by  $E_0 = 500\text{ V} - (183)(1.5)\text{ V} = +225\text{ V}$ .

The capacitor gauge calibration curve from Figure 2 is

$$C(x) = 4.695 + \frac{0.4045}{x} - \frac{0.0074}{x^2} + \frac{0.0010}{x^3}, \quad (2)$$

where  $C(x)$  is in picofarads and  $x$  is in millimeters. The specimen free-surface velocity can be obtained from the equation,

$$U_{fs}(t) = -\frac{dx}{dt} = -\left(\frac{dC}{dt}\right) / \left(\frac{dC}{dx}\right). \quad (3)$$

Substituting  $\frac{dC}{dt}$  from Equation (1) into Equation (3) gives

$$U_{fs}(t) = \frac{0.08889 V(t)}{\frac{dC}{dx}}, \quad (4)$$

where  $V(t)$  is in millivolts,  $\frac{dC}{dx}$  is in picofarads per millimeter, and  $U_{fs}$  is in millimeters per microsecond or kilometers per second.  $\frac{dC}{dx}$  is obtained from Equation (2);

$$\frac{dC}{dx} = -\frac{0.4045}{x^2} + \frac{0.0148}{x^3} - \frac{0.0030}{x^4}. \quad (5)$$

To find the free-surface velocity  $U_{fs}$  from Equations (4) and (5), it is first necessary to find the free-surface position  $x$ . Integrating Equation (1) gives

$$C(x) = C_0 - \frac{1}{RE_0} \int_0^t V dt, \quad (6)$$

where  $x_0$  is the initial specimen spacing and  $C_0 = C(x_0)$ . Substituting  $C(x)$  from Equation (2) and the parameters  $x_0 = 0.259$  mm,  $C_0 = 6.204$  pF,  $R = 50.0 \Omega$ , and  $E_0 = 225$  V into Equation (6) gives

$$\frac{0.0010}{x^3} - \frac{0.0074}{x^2} + \frac{0.4045}{x} = 1.509 - 0.08889 \int_0^t V dt, \quad (7)$$

where  $x$  is the free-surface position in millimeters and  $\int_0^t V dt$  is the area under the voltage-time pulse in millivolt-microseconds. This cubic equation is solved for each voltage-time integral value to find  $x$  as a function of time.

To obtain  $x$  and  $U_{fs}$ , an enlarged photograph was made of the capacitor gauge oscilloscope trace shown in Figure 5(b). The voltage-time pulse was digitized from this photograph. The area under the voltage-time pulse was obtained for selected times by cutting the photograph into pieces and weighing each piece. A standard-grid piece was weighed for calibration. This information was used with Equations (4), (5), and (7) to obtain  $x$  and  $U_{fs}$ . Table 2 gives the results of the computation. The estimated uncertainty in the values is a few percent.

The  $x$  values in Table 2 decrease from 0.259 to 0.157 mm. This range corresponds to the initial portion of the calibration curve in Figure 2 which can be approximated with a straight line. A straight-line least-squares fit of the initial 15 data points in Table 1 gives  $C(x) = 4.615 + 0.4099/x$  for the capacitor gauge calibration curve for this region. When this calibration curve was used in the computation, the  $x$  and  $U_{fs}$  values differed from those in Table 2 by only a few percent.

Figure 6 is a plot of the digitized free-surface-velocity data of Table 2. This profile shows stress reverberations in the tantalum specimen. The initial compressive wave consists of an elastic wave of amplitude 0.061 km/s followed by a plastic wave of slightly larger amplitude. The initial compressive wave is followed by a tensile wave and then a second compressive wave with an

**Table 2. Digitized capacitor gauge voltage data and the corresponding free-surface-position and free-surface-velocity results for tantalum.**

Time <sup>a</sup>	Voltage <sup>a</sup>	Voltage-Time Integral <sup>b</sup> $\int_0^t V dt$	Free-Surface Position <sup>b</sup>	Capacitance Position- Derivative <sup>c</sup> $\frac{dC}{dx}$	Free-Surface Velocity <sup>d</sup>
t ( $\mu s$ )	V (mV)	(mV $\mu s$ )	x (mm)	(pF/mm)	U <sub>fs</sub> (km/s)
0.00	0.00	0.00	0.259	-5.84	0.0000
0.07	-4.04	-0.14	0.257	-5.95	0.0604
0.13	-4.23	-0.37	0.254	-6.11	0.0615
0.17	-4.33	-0.60	0.250	-6.29	0.0612
0.27	-4.23	-1.02	0.244	-6.60	0.0570
0.32	-4.34	-1.22	0.242	-6.75	0.0572
0.37	-4.46	-1.42	0.239	-6.91	0.0574
0.47	-4.72	-1.90	0.233	-7.29	0.0575
0.57	-5.12	-2.38	0.227	-7.69	0.0592
0.62	-5.65	-2.93	0.221	-8.15	0.0617
0.76	-6.16	-3.52	0.215	-8.67	0.0631
0.83	-6.25	-3.86	0.212	-8.97	0.0619
0.87	-5.10	-4.12	0.209	-9.21	0.0492
0.92	-2.77	-4.32	0.207	-9.39	0.0262
0.98	-1.44	-4.40	0.206	-9.47	0.0135
1.03	-0.77	-4.45	0.206	-9.51	0.0072
1.07	-0.63	-4.48	0.206	-9.54	0.0059
1.27	-0.38	-4.57	0.205	-9.63	0.0035
1.47	-0.35	-4.65	0.204	-9.70	0.0032
1.67	-0.35	-4.73	0.203	-9.78	0.0032
1.77	-0.35	-4.77	0.203	-9.82	0.0032
1.83	-1.19	-4.82	0.203	-9.86	0.0107
1.88	-3.10	-4.91	0.202	-9.95	0.0277
1.92	-4.44	-5.10	0.200	-10.1	0.0389
1.97	-5.15	-5.34	0.198	-10.4	0.0441
2.07	-5.77	-5.88	0.193	-10.9	0.0470
2.17	-6.31	-6.50	0.189	-11.5	0.0486
2.28	-6.92	-7.18	0.183	-12.3	0.0501
2.37	-7.58	-7.93	0.178	-13.1	0.0514
2.48	-8.27	-8.75	0.173	-14.0	0.0524
2.55	-8.65	-9.33	0.169	-14.7	0.0522
2.61	-8.90	-9.90	0.166	-15.4	0.0513
2.66	-8.08	-10.31	0.164	-15.9	0.0451
2.72	-5.19	-10.69	0.161	-16.4	0.0281
2.78	-3.15	-10.92	0.160	-16.7	0.0168
2.84	-2.12	-11.09	0.159	-16.9	0.0111
2.91	-1.50	-11.21	0.159	-17.1	0.0079
2.98	-1.25	-11.30	0.158	-17.2	0.0065
3.05	-1.10	-11.38	0.158	-17.3	0.0056
3.12	-1.12	-11.46	0.157	-17.4	0.0057

<sup>a</sup>These values were obtained from the capacitor gauge voltage record shown in Figure 5.

<sup>b</sup>Obtained by solving the cubic Equation (7) for each voltage-time integral value.

<sup>c</sup>Obtained from Equation (5) for each free-surface-position value.

<sup>d</sup>Obtained from Equation (4).

amplitude of approximately 0.05 km/s. The time duration of each of the waves is approximately 0.9  $\mu$ s. The flat, low-amplitude tensile region (no signal reversal) suggests that no spall fracture occurred during the tensile portion of the wave. Taylor reported a pullback velocity (decrease in the free-surface velocity at first wave reversal) for spall fracture of 0.12 km/s for a 1.5- $\mu$ s-wide compressive pulse in tantalum.<sup>6</sup> Isbell et al. obtained a pullback velocity for spall of 0.19 km/s for a 0.8- $\mu$ s-wide compressive pulse in tantalum.<sup>7</sup> These reported values are larger than the 0.06-km/s pullback velocity for the 0.9- $\mu$ s-wide compressive pulse in Figure 6.

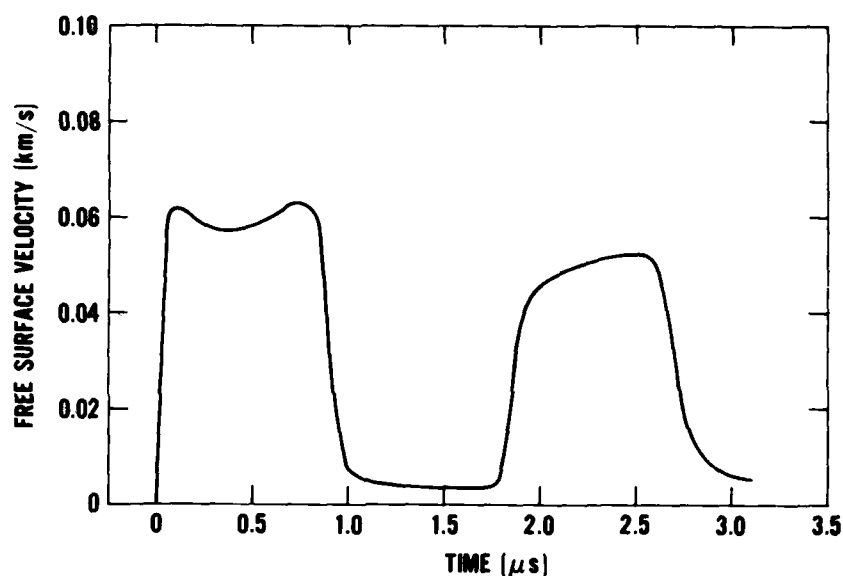


**Figure 6. Free-surface-velocity profile for the 3.73-mm-thick tantalum specimen impacted at 0.111 km/s with a 2.65-mm-thick alpha titanium impactor.**

Table 3 summarizes the shock wave results for tantalum. The measured 4.15-km/s elastic wave velocity is the same as the ultrasonic longitudinal wave velocity reported by Isbell et al.<sup>7</sup> The elastic wave particle velocity value of 0.031 km/s is in good agreement with the 0.029-km/s value reported by Isbell et al.<sup>7</sup> The 2.1-GPa Hugoniot elastic limit value is slightly larger than the 1.8-GPa value for a propagation distance of 3.8 mm reported by Isbell et al.<sup>7</sup> Using the reported stress - particle-velocity relationships for alpha titanium<sup>8</sup> ( $\sigma_H = 0.25 + 22.5 u_p + 4.99 u_p^2$ ,

Table 3. Summary of shock-wave results for tantalum.

Shot No.	Description of Shot	Impactor		Initial		Specimen Thickness (mm)	Specimen Diameter (mm)	Specimen Density $\rho_0$ (Mg/m <sup>3</sup> )	Projectile Velocity <sup>a</sup> $U_0$ (km/s)	Impactor Tilt (mrad)
		Diameter (mm)	Thickness (mm)	Impactor Density (Mg/m <sup>3</sup> )	Impactor Thickness (mm)					
172	Ti-Ta/tilt pins, capacitor gauge	35.60	2.65	4.50		3.73	27.99	16.60	0.111	0.35

Elastic Wave						Plastic Wave			
Shot No.	Wave Velocity <sup>b</sup> $U_e$ (km/s)	Particle Velocity <sup>c</sup> $u_e$ (km/s)	Stress <sup>d</sup> $\sigma_e$ (GPa)	Strain <sup>e</sup> $\Delta V_e/V_0$		Wave Velocity <sup>b</sup> $U_s$ (km/s)	Particle Velocity <sup>f</sup> $u_p$ (km/s)	Stress <sup>g</sup> $\sigma_H$ (GPa)	Strain <sup>h</sup> $\Delta V/V_0$
172	4.15	0.0307	2.11	0.0074		3.19	0.0316	2.16	0.0077

<sup>a</sup>Average of three measurements. The estimated uncertainty is 0.5%.

<sup>b</sup>Calculated using the measured elastic and plastic wave transit times through the specimen disk. The elastic wave transit time was obtained using the first-signal value for the initial-free-surface velocity pulse. The plastic wave transit time was obtained using the minimum free-surface-velocity value immediately following the elastic portion of the initial free-surface-velocity pulse. The estimated wave velocity uncertainty is 5%.

<sup>c</sup>Taken as one half the maximum free-surface-velocity value of the elastic wave.

<sup>d</sup> $\sigma_e = \rho_0 U_e u_e$

<sup>e</sup> $\Delta V_e/V_0 = 1 - V_e/V_0 = u_e/U_e$  where  $V_0 = 1/\rho_0$ .

<sup>f</sup>Taken as one half the maximum free-surface-velocity value of the plastic wave.

<sup>g</sup> $\sigma_H = \sigma_e + \rho_0 (U_s - u_e) (u_p - u_e)$  where  $\rho_e = \rho_0 / (1 - u_e/U_e)$ .

<sup>h</sup> $\Delta V/V_0 = 1 - V/V_0$  where  $V/V_0 = (1 - u_e/U_e)(U_s - u_p)/(U_s - u_e)$  and  $V = 1/\rho$ .

$\sigma_H < 9$  GPa,  $u_p$  in km/s) and tantalum<sup>7</sup> ( $\sigma_H = 0.4 + 55.0 u_p + 21.5 u_p^2$ ,  $\sigma_H < 20$  GPa,  $u_p$  in km/s) gives an initial stress and particle velocity of 2.1 GPa and 0.031 km/s, respectively, for alpha titanium impacting tantalum at 0.111 km/s. These values are in good agreement with the measured 2.2-GPa stress and 0.032-km/s particle velocity for the plastic wave in Table 3. The measured 3.19-km/s shock wave velocity in Table 3 is slightly less than a calculated value of 3.40 km/s obtained from the tantalum shock-velocity - particle-velocity relationship<sup>7</sup>  $U_s = 3.36 + 1.24 u_p$ .

After shock loading, the recovered tantalum specimen was sectioned on a diameter and polished. Figure 7 is a photograph of this surface. No fracture damage was revealed by microscopic observation. An initial tensile pulse amplitude of about 2 GPa is estimated for this specimen based on the shock compression results of Table 3. This value is less than the 4.4- and 6.8-GPa spall strength values that have been reported for tantalum.<sup>2,7</sup>

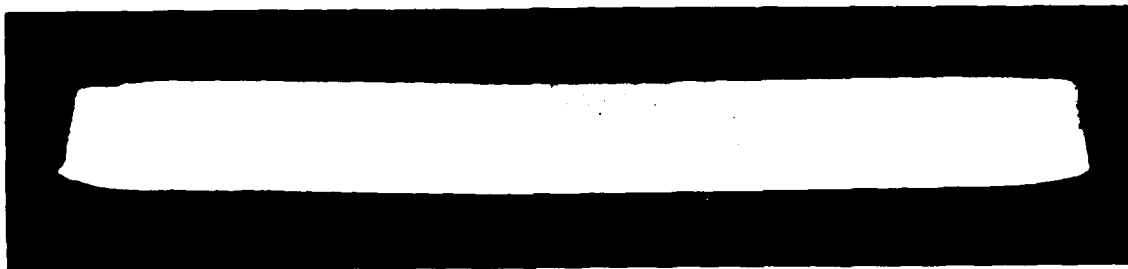


Figure 7. Photograph of the recovered, sectioned, and polished shock-loaded tantalum specimen. The bottom edge of the disk is the impact surface.

#### IV. SUMMARY

The free-surface velocity of a shock-loaded tantalum disk has been measured. Stress reverberations were produced in the disk by impacting it with an alpha titanium disk at a velocity of 0.111 km/s. The tensile pulse amplitude and duration were less than that required for spall fracture in the tantalum disk. The shock wave measurements agree with the results of previous work.

## REFERENCES

1. W. Mock, Jr. and W. H. Holt, *Capacitor Gauge for Gas Gun Experiments*, NSWC TR 79-192, Naval Surface Weapons Center, Dahlgren, VA 22448 (June 1979).
2. S. Cochran and D. L. Banner, "Spall Studies in Uranium," *Journal of Applied Physics*, Vol. 48, p. 2729 (1977).
3. W. Mock, Jr. and W. H. Holt, *The NSWC Gas Gun Facility for Shock Effects in Materials*, NSWC TR-3473, Naval Surface Weapons Center, Dahlgren, VA 22448 (July 1976).
4. The materials and hardness measurements were provided by D. R. Coltharp, Army Waterways Experiment Station, Corps of Engineers, P.O. Box 631, Vicksburg, MS 39180.
5. M. H. Rice, "Capacitor Technique for Measuring the Velocity of a Plane Conducting Surface," *The Review of Scientific Instruments*, Vol. 32, p. 409 (1961).
6. J. W. Taylor, "Stress Wave Profiles in Several Metals," *Dislocation Dynamics*, McGraw-Hill Book Co., New York, NY, p. 573 (1968).
7. W. M. Isbell, D. R. Christman, and S. G. Babcock, *Measurements of Dynamic Properties of Materials, Vol. VI, Tantalum*, General Motors Technical Center Report DASA 2501-6, Warren, MI (February 1972).
8. D. R. Christman, T. E. Michaels, W. M. Isbell, and S. G. Babcock, *Measurements of Dynamic Properties of Materials, Vol. IV, Alpha Titanium*, General Motors Technical Center Report DASA 2501-4, Warren, MI (February 1972).

## DISTRUBUTION

Commander  
Naval Sea Systems Command  
Washington, DC 20360  
ATTN: SEA-003 (S. R. Marcus)  
SEA-05R (G. N. Sorkin)  
SEA-05R22 (S. J. Matesky)  
SEA-62R (W. W. Blaine)  
SEA-62R31 (R. A. Bailey)  
SEA-62R32 (G. Edwards)  
SEA-62R54 (B. Lubin)  
SEA-62Y13C (L. H. Hawver)  
SEA-62Z3 (J. Whelan)  
SEA-62R4 (M. A. Kinna)

Commander  
Naval Air Systems Command  
Washington, DC 20360  
ATTN: AIR-310 (H. J. Mueller)  
AIR-310B (J. W. Willis)  
AIR-320 (T. F. Kearns)  
AIR-350 (H. B. Benefiel)  
AIR-5163 (C. Bersch)  
AIR-5324 (S. Englander)

Office of Naval Research  
Department of the Navy  
Washington, DC 20360  
ATTN: ONR-420 (T. G. Berlincourt)  
ONR-465 (E. I. Salkovitz)

Office of Naval Research  
536 S. Clark St.  
Chicago, IL 60605  
ATTN: George Sandoz

Office of Naval Research  
Bldg. 114 Section D  
666 Summer St.  
Boston, MA 02210  
ATTN: L. H. Peebles, Jr.



**DISTRIBUTION (Continued)**

Commander  
Naval Research Laboratory  
Washington, DC 20375  
ATTN: 7908 (A. Williams)

Commander  
Naval Weapons Center  
China Lake, CA 93555  
ATTN: M. E. Backman  
R. L. Ballenger  
J. Pearson  
H. Pieper  
E. B. Royce  
R. G. Sewell  
T. Zulkoski

Director  
Army Ballistics Research Laboratories  
Terminal Ballistics Laboratory  
Aberdeen Proving Ground, MD 20015  
ATTN: W. S. deRosset  
W. Gillich  
G. E. Hauver  
G. Moss  
R. Vitali

Commander  
Army Materials and Mechanics Research Center  
Watertown, MA 02172  
ATTN: D. T. Dandekar  
J. F. Mescall

Commander  
Army Research and Development Command  
Dover, NJ 07801  
ATTN: F. J. Owens

Commander  
Army Engineer Waterways Experiment Station  
Corps of Engineers  
Vicksburg, MS 39180  
ATTN: D. R. Coltharp

**DISTRIBUTION (Continued)**

Los Alamos Scientific Laboratory  
Los Alamos, NM 87544  
ATTN: J. M. Holt, Jr.  
R. Morales  
J. A. Morgan  
Technical Library

(2)

Sandia Laboratories  
Albuquerque, NM 87115  
ATTN: Lee Davison  
R. A. Graham  
Technical Library

(2)

Lawrence Livermore Laboratory  
University of California  
Livermore, CA 94550  
ATTN: S. Cochran  
W. H. Gust  
E. Nidick, Jr.

New Mexico Institute of Mining and Technology  
Campus Station  
Socorro, NM 87801  
ATTN: P. D. Buckley  
H. L. Giclas  
M. L. Kempton

SRI International  
333 Ravenswood Avenue  
Menlo Park, CA 94025  
ATTN: D. Curran  
L. Seaman

Shock Dynamics Laboratory  
Washington State University  
Pullman, WA 99163  
ATTN: G. E. Duvall  
G. R. Fowles

**DISTRIBUTION (Continued)**

GIDEP Operations Office  
Corona, CA 91720

Defense Technical Information Center  
Cameron Station  
Alexandria, VA 22314

(12)

Defense Printing Service  
Washington Navy Yard  
Washington, DC 20374

Library of Congress  
Washington, DC 20540  
ATTN: Gift and Exchange Division

(4)

**Local:**

C  
D  
E41  
F  
F10  
F12 (Berger)  
G  
G10  
G102  
G103  
G13  
G13 (Wasmund)  
G13 (Hock)  
G13 (Dickinson)  
G20  
G30  
G301  
G302  
G31  
G32  
G33  
G34  
G34 (Bolt)  
G34 (Hales)

**DISTRIBUTION (Continued)**

G34 (D. Smith)  
G34 (T. Smith)  
G35  
G35 (Elliott)  
G35 (Mock)  
G35 (Holt)  
G35 (Wishard)  
G35 (Waggener)  
G40  
G50  
G60  
K21  
K21 (Blackmon)  
R  
R04  
R10  
R12 (Erkman)  
R13  
R13 (Coleburn)  
R13 (Forbes)  
R13 (Roslund)  
R30  
R32  
X210

(6)